TEORIJSKA I PRIMENJENA MEHANIKA 19, pp 73–85, 1993, UDK 533.6

SOLUTION OF THE EULER EQUATIONS ON UNSTRUCTURED GRIDS FOR STEADY TWO–DIMENSIONAL FLOWS

M.S. Kozić

(Received 30.08.1993)

1. Introduction

During the last two decades considerable progress has been made on developing computational fluid dynamics (CFD) methods for aerodynamic analysis [1]. Panel methods for subsonic flow were introduced in the sixties [2, 3], the seventies have seen major advances in the simulation of transonic flow by the potential flow approximation [4–7], and recent work has focused in solving the Euler and Navier–Stokes equations [8–12].

The development of a suitable method for mesh generation is main problem involved with analysis of complex geometry. For simple wing–body configurations it is not too difficult to generate rectilinear meshes [8], but it becomes increasingly difficult to generate a structured mesh that is aligned with all solid surfaces, for complicated combinations consisting of wing–body–tail–fin. Generation of structured rectilinear mesh about complete aircraft with pylon mounted engines, poses extremely severe problems for any such method. An alternative to overcome these problems is to use unstructured mesh [7]. In this approach the grid generation techniques involve the use of triangular cells and the grid points can be distributed using a suitable algorithm.

In this paper, algorithm developed in [18] for the solution of two–dimensional Euler equations is described. The algorithm was developed for steady flow analysis about multiple two–dimensional bodies, using unstructured grid consisted of triangles. The flow algorithm solves the time–dependent integral form of the equations by means of a cell–centered finite–volume discretisation. The integration in time is performed using an explicit Runge–Kutta time–stepping scheme. The solver uses explicitly added artificial dissipation to prevent spurious oscillations near shock waves and to damp high frequency uncoupled error modes.

2. Mesh generation

Generation of an unstructured grid can be divided in two independent steps. A set of points is first generated around complete configuration, and these points are then jointed to form a tessellation by triangles. This connection is non–unique, but it is always possible to join the points so that the circle through the three points forming any triangle contains no other points. This unique tessellation is known as the Delaunay triangulation [13].

The geometric dual of the Delaunay triangulation is the Voronoi diagram [14] which assigns to each node the territory of the domain which is closer to that node than any other node in the set. The boundary of the Voronoi neighborhood is formed from segments of the bisectors of the lines joining a point P_i to each of the surrounding points. This is illustrated in Fig. 1. A vertex of the Voronoi diagram is formed where three edges meet.

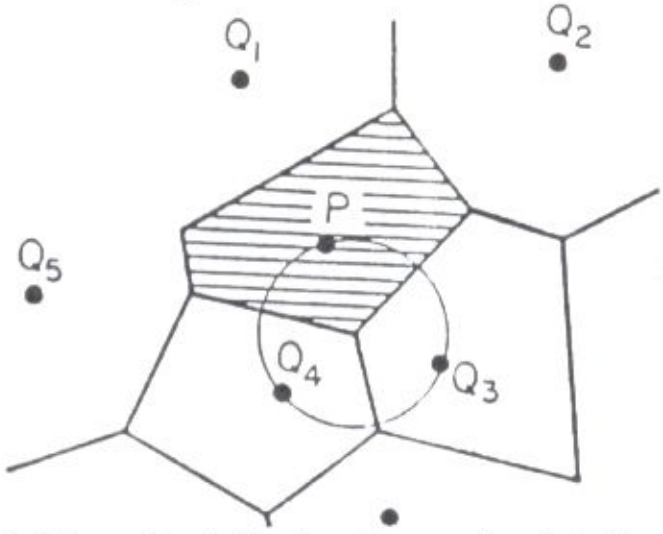

Fig. 1. Voronoi neighborhood around point P

Since each edge of the Voronoi diagram is equidistant from two points, a vertex is equidistant from three points and is circumcenter of the circle passing through the three points. The Delaunay triangulation is obtained by joining each point to its neighbor across each edge of the Voronoi diagram, Fig. 2.

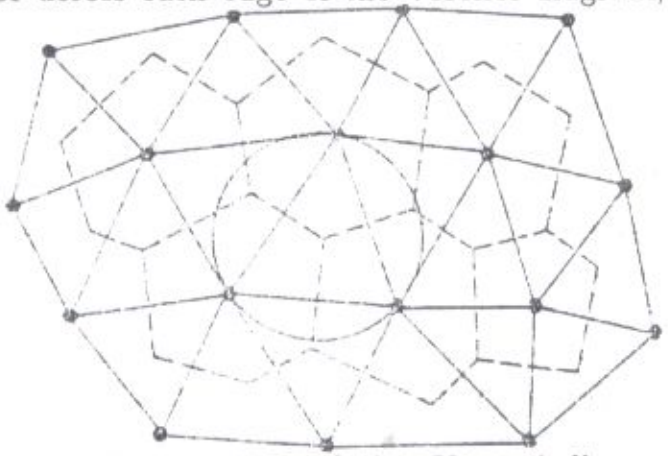

Fig. 2. Delaunay triangulation Voronoi diagram

A straightforward method for generating the Delaunay triangulation is Bowyer's algorithm [15] which sequentially constructs an existing Delaunay triangulation. All triangles whose circumcircles contain the new node must be removed because they violate Delaunay triangulation. The resulting convex cavity obtained in this way must be retriangulated in such a manner that the new triangulation is again Delaunay. This process is shown in Fig. 3.

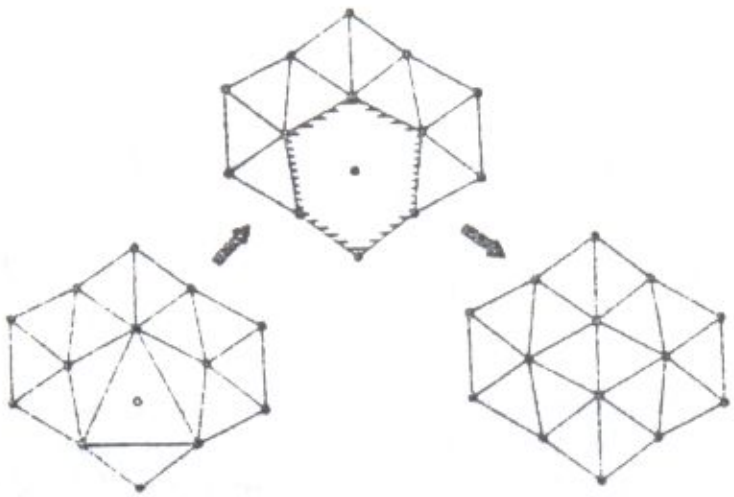

Fig. 3. Bowyer's algorithm

A new node is added in a Delaunay triangulation. Now the circumcircles of the large triangle and its three neighboring triangles contain the new node and these four triangles violate Delaunay triangulation. A convex cavity is obtained removing these triangles from domain, so that all boundary nodes of the cavity are visable to the new node. Connection of the new node with all nodes of the cavity boundary completes the triangulation which is again Delaunay, and Bowyer's algorithm is prepared for the next node to be introduced.

The efficiency of Bowyer's procedure is dependent on the time to search the first circumcircle which contains the new node, all remaining circumcircles are easily found by tree search. The set of point is in general randomly orderd, a simple search would require $O(N)$ operations to locate the first containing circumcircle for each node, leading to $O(N^2)$ operations for complete triangulation. It is necessary to use a data structure that allows an efficient search for the first triangle that violates Delaunay triangulation, no matter of the points ordering. A quadtree structure [16] have been used to store the points that have previously been inserted. In this way the final triangulation can be reduced to $O(N \log N)$ operations.

3. Governing equations and spatial discretization

Two–dimensional flow of an inviscid fluid in a domain Ω with boundary $\partial\Omega$ is described by the Euler equations in integral form

$$\frac{\partial}{\partial t}\iint_{\Omega} W\,\mathrm{d}x\,\mathrm{d}y + \int_{\partial\Omega}(F\,\mathrm{d}y - G\,\mathrm{d}x) = 0, \tag{1}$$

where the vector of conserved variables W and the convective fluxes F and G are given by

$$W = \begin{pmatrix} \rho \\ \rho u \\ \rho v \\ \rho E \end{pmatrix}, \quad F = \begin{pmatrix} \rho u \\ \rho uu + p \\ \rho vu \\ \rho uH \end{pmatrix}, \quad G = \begin{pmatrix} \rho v \\ \rho uv \\ \rho vv + p \\ \rho vH \end{pmatrix}, \tag{2}$$

where ρ, p, u, v, H i E are density, pressure, the Cartesian velocity components, total enthalpy per unit mass and total energy per unit mass, respectively. These quantities are related to each other by the definitions of total energy and total enthalpy per unit volume for a perfect gas

$$\rho E = \frac{p}{\gamma - 1} + \rho\frac{u^2 + v^2}{2} \tag{3}$$

$$\rho H = \rho E + p \tag{4}$$

The computational domain is divided into a finite number of triangles Fig. 4, and the integral conservation equations are applied to each cell. The conserved variables are assumed to be constant within a cell, and it leads to a system of ordinary differential equations with respect to time

$$\frac{\mathrm{d}}{\mathrm{d}t}(S_i W_i) + Q(W_i) = 0, \quad i = 1, 2, \ldots, N \tag{5}$$

where $Q(W_i)$ is a discrete approximation of the flux integral, given by

$$Q(W_i) = \sum_{m=1}^{3}(F\Delta y - G\Delta x)_m = 0 \tag{6}$$

and summation is over the edges forming the $i-th$ cell.

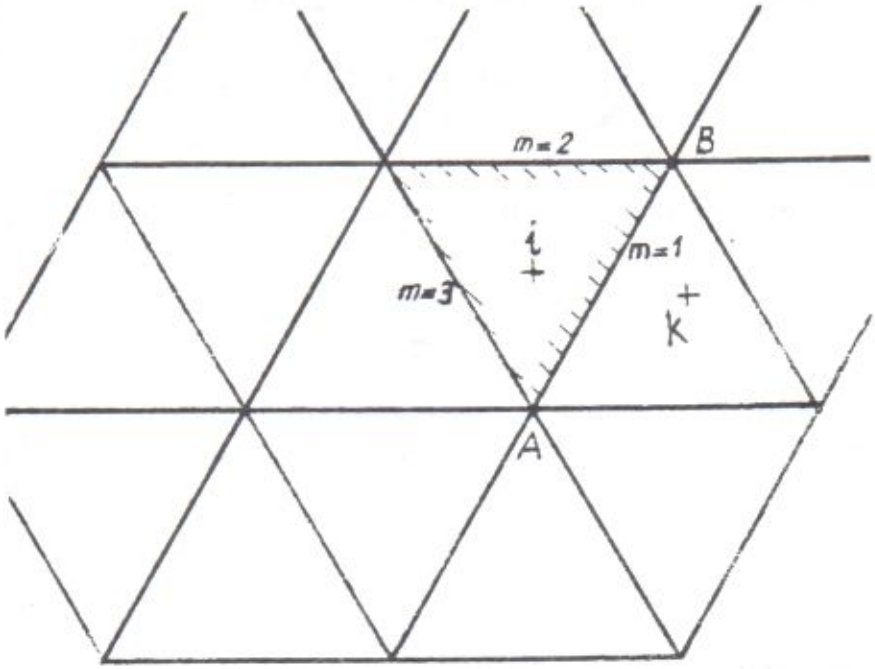

Fig. 4 Triangular cell as a control volume

The flux vectors are taken to be the averages of the values in the cells on either side of the edge. The $x-$ momentum flux components are given by

$$f_m = \frac{(\rho u^2 + p)_i + (\rho u^2 + p)_k}{2} \tag{7a}$$

$$g_m = \frac{(\rho uv)_i + (\rho uv)_k}{2} \tag{7b}$$

4. Artificial dissipation

Dissipative terms have to be added to discretized form of the unsteady Euler equations, which are a set of nondissipative hyperbolic conservation laws, to prevent oscillations near shock waves and to damp high frequency uncoupled error modes. Adding these terms, equation (5) becomes

$$\frac{\mathrm{d}}{\mathrm{d}t}(S_i W_i) + Q(W_i) - D(W_i) = 0, \quad i = 1, 2, \ldots, N \tag{8}$$

In the present work the approach of Jameson and coworkers [8] is used, and the dissipation function $D(W_i)$ is constructed as a blending of second and fourth differences of the conserved variables. The biharmonic operator provides a background dissipation to damp high frequency errors and it is switched–off in the region of shock waves. The harmonic operator prevents oscillations near shocks, and is switched–on near shock waves. By the analogy with structured grids the artificial dissipative terms are constructed for unstructured grids, by summation of the dissipative fluxes across the edges of a triangular element

$$D(W_i) = \sum_{m=1}^{3} d_m^{(2)} + \sum_{m=1}^{3} d_m^{(4)}, \tag{9}$$

where the second and fourth differences are given by

$$d_m^{(2)} = \alpha_m \epsilon_m^{(2)} (w_k - w_i)_m , \tag{10a}$$

$$d_m^{(4)} = -\alpha_m \epsilon_m^{(4)} (\Delta w_k - \Delta w_i)_m , \tag{10b}$$

Index m denotes the common edge between cells i and k, and Δ is defined as

$$\Delta w_i = \sum_{k=1}^{3} (w_k - w_i) . \tag{11}$$

The scaling factor α_m depends on the maximum eigenvalues of Jacobian matrices $\partial F/\partial W$, and $\partial G/\partial W$ along the appropriate edge, and is given by

$$\alpha = |u\Delta y - v\Delta x| + a\Delta l \tag{12}$$

where u, v, and a are average values on $m-th$ edge, a being the local speed of sound. The values of adaptive coefficients $\epsilon^{(2)}$ and $\epsilon^{(4)}$ are based on local pressure gradient given by shock sensor

$$\nu_i = \frac{\left| \sum_{m=1}^{3} (p_k - p_i)_m \right|}{\left| \sum_{m=1}^{3} (p_k + p_i)_m \right|} . \tag{13}$$

Finally, the resulting adaptive coefficients are

$$\epsilon_m^{(2)} = K^{(2)} \max \left[(\nu_i, \nu_k)_m \right] , \tag{14a}$$

$$\epsilon_m^{(4)} = \max \left(0,\ K^{(4)} - \epsilon_m^{(2)} \right) \tag{14b}$$

where $K^{(2)}$ and $K^{(4)}$ are two empirically determined constants with the values $0.5 \leq K^{(2)} \leq 1.0$, $1/256 \leq K^{(4)} \leq 1/32$.

Correct treatment of the dissipation near boundaries is necessary for obtaining accurate solutions. If the dissipation terms added to damp oscillations of solution are too strong, the order of the numerical scheme can be reduced and a large amount of spurious numerical entropy is produced near the boundary. This causes the total pressure losses on the surface of the airfoil. In the present work the approach from [17] is applied, by simply setting equal to zero the contributions from the boundary edges.

5. Time integration

The spatial discretization of the Euler equations leads to a set of coupled ordinary differential equations with respect to time

$$\frac{\mathrm{d}W_i}{\mathrm{d}t} + R(W_i) = 0, \quad i = 1, 2, \ldots, N \tag{15}$$

where $R(W_i)$ is the vector of the residuals consisting of the flux balance of conserved variables together with the added dissipative terms. These equations are to be integrated until they reach a steady state. For this purpose the integration in time is performed using an explicit Runge–Kutta four–stage time stepping scheme given by

$$\begin{aligned} W_i^{(0)} &= W_i^n \\ W_i^{(m)} &= W_i^{(0)} + \alpha_m \Delta t \, R_i^{(m-1)} \quad \text{for} \quad m = 1 \text{ to } 4 \\ &\vdots \qquad\qquad\qquad\qquad i = 1, 2, \ldots, N. \\ W_i^{n+1} &= W_i^{(4)} \end{aligned} \tag{16}$$

where n is the current time level, $n+1$ is the new time level. Residual and coefficients are given by

$$R_i^{(m)} = \frac{\left(Q_i^{(m)} - D_i^{(0)}\right)}{S_i} \tag{17}$$

$$\alpha_1 = \frac{1}{4}, \quad \alpha_2 = \frac{1}{3}, \quad \alpha_3 = \frac{1}{2}, \quad \alpha_4 = 1. \tag{18}$$

Because of computational efficiency, the dissipative term is evaluated only at the first stage. The scheme represented by equation (16) is second–order accurate in time. The allowable time step in explicit schemes of this type is restricted because of the limited stability region and for multi–dimensional system of equations can be evaluated only in an approximate way.

6. Boundary conditions

A condition of flow tangency is applied at solid boundaries, simply setting the normal velocity flux accros the boundary to be equal to zero. The x and y momentum fluxes are not equal to zero due to pressure terms. The pressure is extrapolated onto the airfoil, and zero–th order extrapolation procedure is used, i.e. the pressure at the solid surface is taken to be equal to the pressure at the centre of the adjacent boundary cell.

In the far field the requirement is that none of the outgoing waves are reflected back into computational domain. A characteristic analysis based on Riemann invariants is used in determination of flow variables on the outer boundary.

7. Results

7.1 NACA 0012 aerofoil

Present method has initially been checked using standard AGARD01 test case for the NACA 0012 aerofoil. The unstructured grid had 3866 nodes, 7452

triangles, and extended 20 chordlengths from the aerofoil with a circular outer boundary. Also there were 110 points distributed on the aerofoil surface. Calculation was performed for the airfoil at a freestream Mach number $M = 0.8$, an angle of attack $\alpha = 1.25^0$, and $CFL = 8.4$. The solution residual was reduced by over four orders of magnitude, as determined by the reduction in the L_2 norm of the density residual.

Calculated pressure distribution is shown in Fig. 5. For this case there is a relatively strong shock wave on the upper surface of the airfoil at around 65% chord, and a weak shock waves on the lower surface at 30% chord.

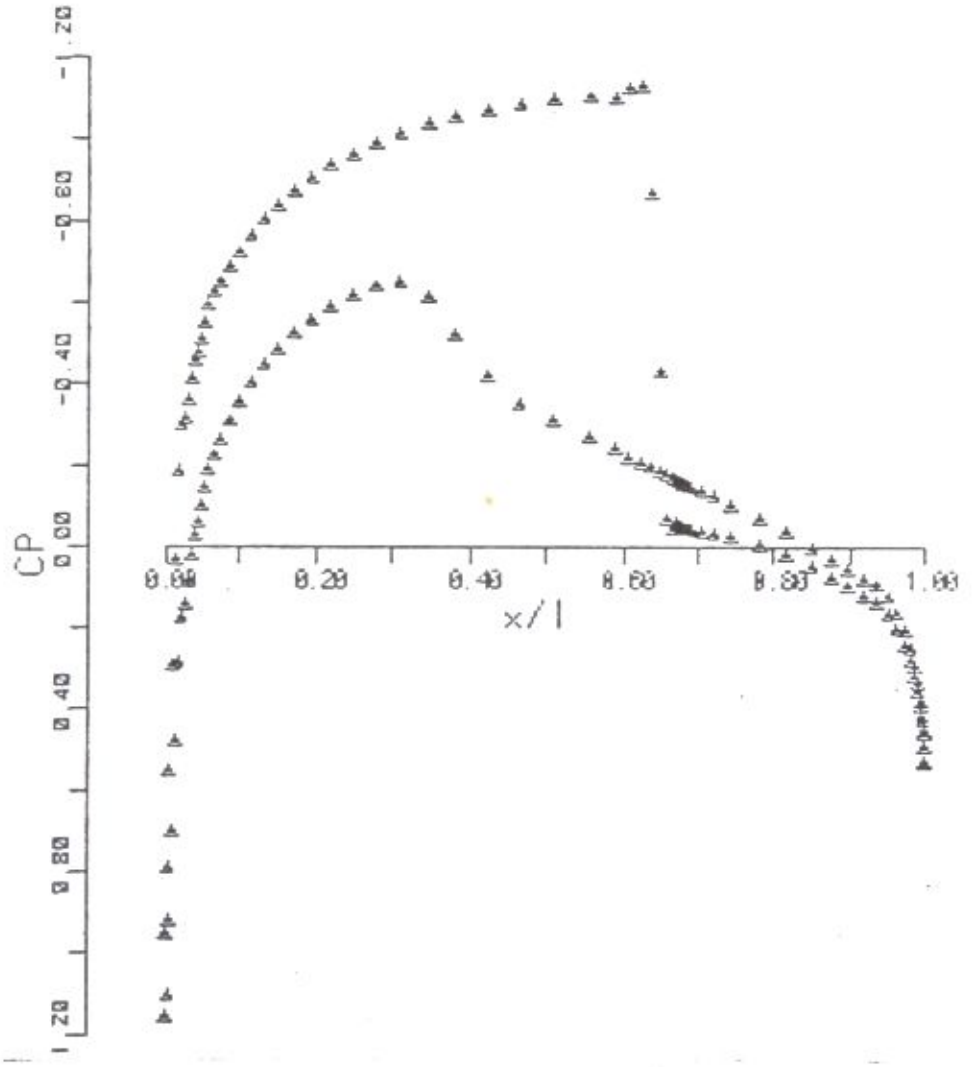

Fig. 5 Surface pressure distribution for the test case AGARD01 (NACA 0012 airfoil, $M = 0.8$, $\alpha = 1.25^0$)

In Table 1. lift and drag coefficients from the present method, are compared with results from a number of existing methods.

Test case : AGARD01 *Airfoil* : NACA 0012 *Mach number* : 0.8 *Angle of att.* : 1.25^0		
	CZ	CX
REF. [22]	0.3436	0.0227
REF. [21] (central differences)	0.3504	0.0227
REF. [21] (TVD scheme)	0.3349	0.0262
REF. [23]	0.3099	0.0168
REF. [20] (optimal scheme)	0.2971	0.0203
REF. [19]	0.3400	0.0230
PRESENT METHOD	0.3186	0.0241

Table 1. Comparison of calculated lift and drag corfficients for the AGARD01 test case

7.2 Multi–element aerofoil

The further validation of the present method has been performed testing inviscid flow around GA(W)–1 aerofoil with extended flap. It is a closely–coupled 2–element aerofoil geometry, and the main problem in calculations with such configurations concerns the generation of a suitable grid because the flow domain is multiply–connected. Fig. 6. shows the computational mesh, consisted of 6897 grid points, forming 13400 cells. There were 130 grid points on the surface of the main aerofoil and 126 on the flap.

The results were obtained using the present method at a freestream Mach number of 0.14, an incidence angle of zero, the flap deflection being 15^0. The surface pressure distribution is compared in Fig. 7 with results from [24], showing good agreement with experimental results. Potential flow calculation results [24] show noticeable deviation in the rear part on the upper surface of the main element.

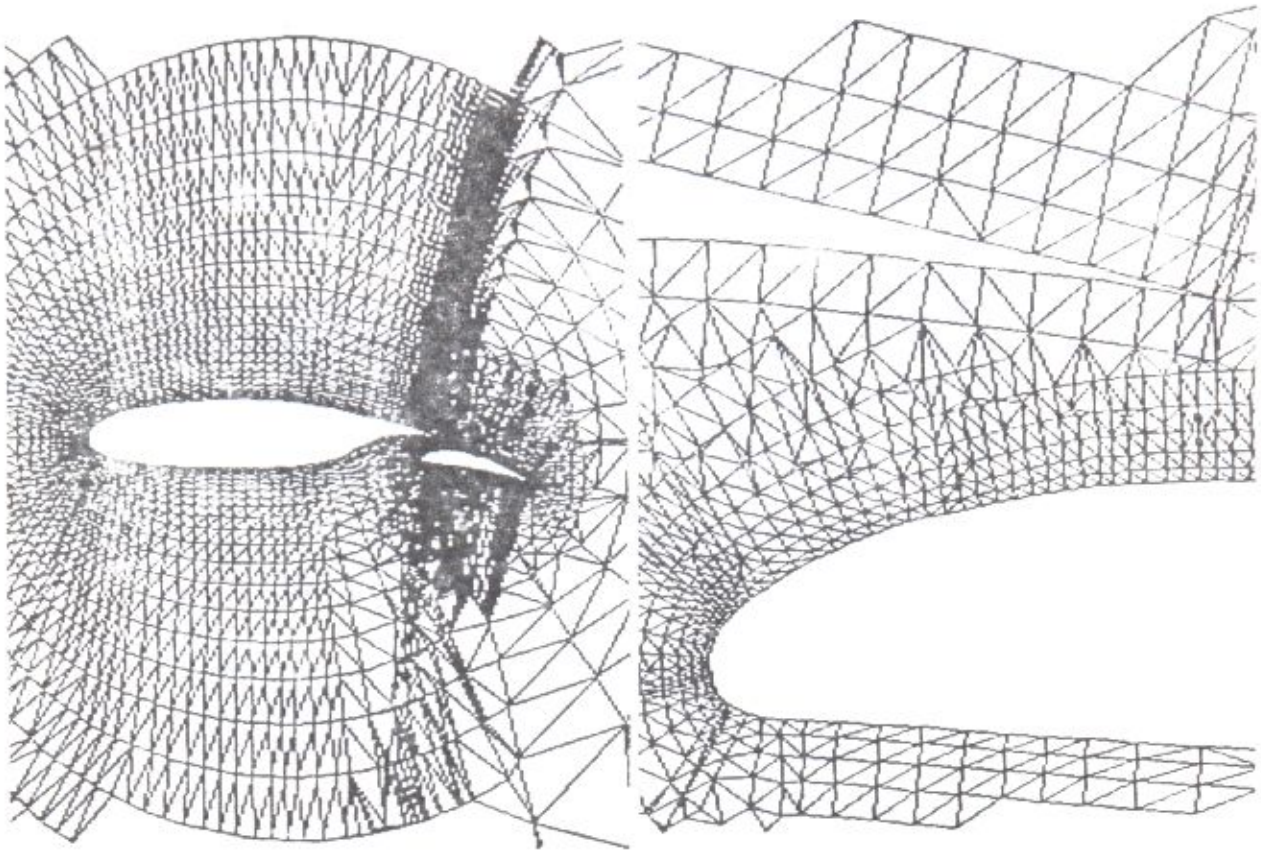

Fig. 6 Partial views of computational mesh for 2-element aerofoil

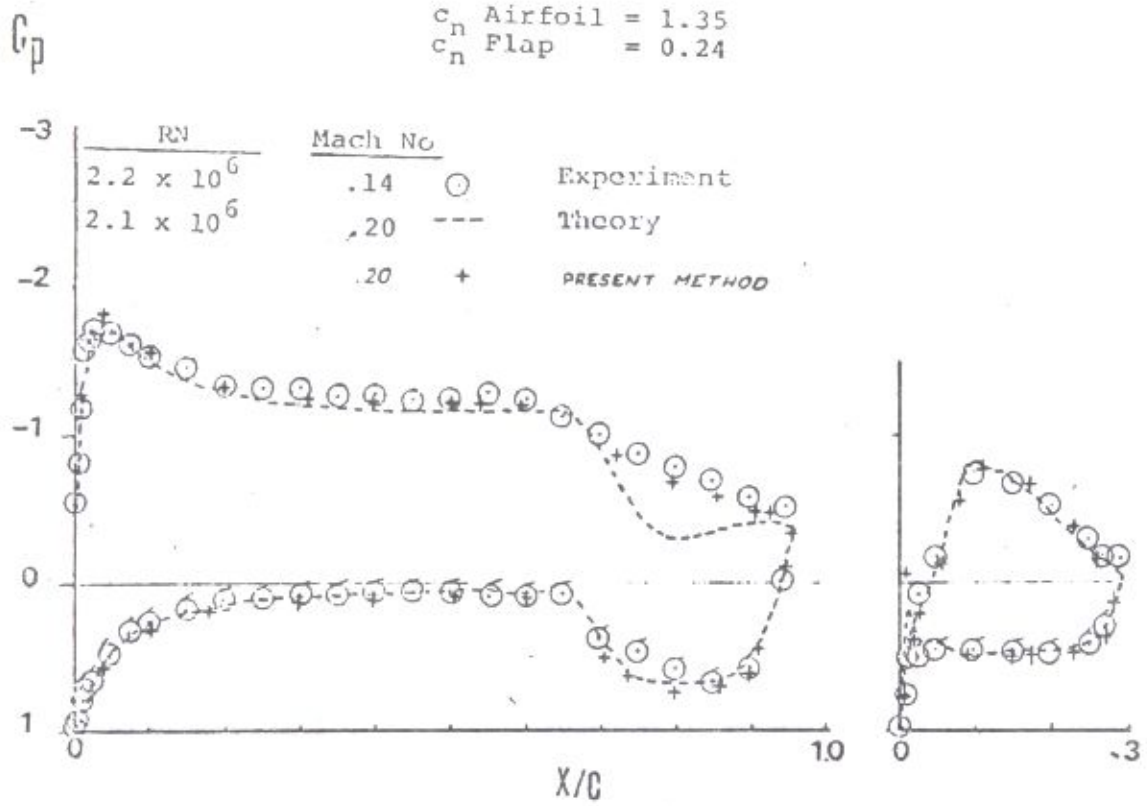

Fig. 7 Surface pressure distribution for 2-element aerofoil

8. Conclusions

A method for the solution of the two–dimensional Euler equations on unstructured grids, has been presented. The method is capable of treating steady subsonic, transonic and supersonic flows about single and multi– element aerofoils.

The steady–state solution is reached by integrating in time the unsteady form of the equations, using an explicit multistage procedure. The convegrence is accelerated using some standard acceleration techniques.

The ability of the present method to treat arbitrary grids and complex geometries has been shown. The mesh adaptive procedures can be introduced without any changes in the basic algorithm.

The unstructured grids can be relatively easily generated around complicated configurations. This fact caused that current development is being directed toward developing three–dimensional flow solver using tetrahedral grids.

REFERENCES

[1] Jameson, A., *Succeses and Challenges in Computational Aerodynamics*, AIAA, **87**, 1184 (1987).

[2] Hess, J.L. and A.M O., Smith, *Calculation of Non–Lifting Potential Flow About Arbitrary Three Dimensional Bodies*, Douglas Aircraft Report **ES 40622**, (1962).

[3] Rubbert, P.E., and G.R. Saaris, *A General Three Dimensional Potential Flow Method Applied to V/STOL Aerodynamics*, SAE Paper **680304**, (1968).

[4] Murman, E.M., and J.D. Cole, *Calculation of plane steady transonic flows*, AIAA Journal **9** (1971), 114–121.

[5] Jameson, A., *Iterative Solution of Transonic Flows Over Airfoils and Wings, Including Flows at Mach 1*, Communications in Pure and Applied Methematics, **27** (1974), 283–389.

[6] Jameson, A., and D.A. Caughey, *A Finite Volume Method for Transonic Potential Flow Calculations*, Proc. AIAA. 3rd Computational Fluid Dynamics Conference, Albuquerque, (1977), 35–54.

[7] Bristeau, M.O., Pironneau, O., Glowinski, R., Periaux, J., Perrier, P., and Poirier, G. *On the Numerical Solution of Nonlinear Problems in Fluid Dynamics by Least Squares and Finite Element Methods (II). Application to Transonic Flow Simulations*, Proc. 3rd International Conference on Finite Elements in Nonlinear Mechanics, FENOMECH 34, Stuttgart, (1984), 363–394, edited by Dotsinis, J.St., Nort Holland, (1985).

[8] Jameson, A., W.Schmidt, and E.Turkel, *Numerical solution of the Euler equations by finite volume method using Runge–Kutta time stepping schemes*, AIAA Paper, **81** (1989), 1259.

[9] Ni, R.H., *A Multiple Grid Scheme for Solving the Euler Equations*, Proc. AIAA. 5th Computational Fluid Dynamics Conference, Palo Alto, (1981), 257–264.

[10] Jameson, A., and T.J. Baker, *Solution of the Euler Equations for Complex Configurations*, Proc. AIAA 6th Computational Fluid Dynamics Conference, Danver, (1983), 293–302.

[11] Pulliam, T.H. and J.L. Steger, *Recent Improvements in Efficiency, Accuracy and Convergence for Implicit Approximate Factorization Algorithms*, AIAA Paper 85–0360, 23rd Aerospace Sciences Meeting, Reno, January (1985).

[12] Mac Cormack, R.W., *Current Status of Numerical Solutions of the Navier–Stokes Equations*, AIAA Paper 85–0032, AIAA 23rd Aerospace Sciences Meeting, Reno, January (1985).

[13] Delaunay, B., *Sur la Sphere vide*, Bull. Acad. Science USSR VII: Class. Sci., Mat. Nat. (1934), 793–800.

[14] Voronoi, G., *Nouvelles Applications des Parametres Continus a la Theorie des Formes Quadratiques. Deuxieme Memorie: Recherches Sur les Parallelloedres Primitifs*, J. Reine Angew. Math. **134** (1908), 198–287.

[15] Bowyer, A., *Computing Dirichlet Tessellations*, The Computer Journal, **24**, No.2, (1981), 162–166.

[16] Lohner, R., *Some useful data structures for the generation of unstructured grids*, Commun. Appl. Num. Meth., **4**, (1988), 123–135.

[17] Stolcis, L., and L.J., Johnston *Solution of the Euler equations on unstructured grids for two-dimensional compressible flow*, Aeronautical Journal, (1990), 181–195.

[18] Kozić, S.M., *Method for Solving Euler equations applied to unsteady two-dimensional transonic flows*, Ph.D.Thesis, Belgrade University (1992).

[19] Schmidt, W., and A. Jameson *Euler solvers as an analysis tool for aircraft aerodynamics*, Advances in computational transonic, ed. W.G., Habashi, (1985), 371–404.

[20] Lerat, A., and J., Sides, *A new finite-volume method for the Euler equations with applications to transonic flows*, Numerical method in aeronautical fluid dynamics, ed. P.L., Roe, (1982), 245–259.

[21] Jameson, A., *Multigrid algorithm for compressible flow calculations*, MAE Report 1743, (1985).

[22] Mavriplis D., *Solution of the two-dimensional Euler equations on unstructured triangular meshes*, Ph.D.Thesis, MAE Dep., Princeton University, June (1987).

[23] Pulliam, T., *Implicit finite difference methods for the Euler equations*, Advances in computational transonic, ed. W.G., Habashi, (1985), 503–542.

[24] Wentz, W.H., and H.C., Seetharam *Development of a Fowler Flap System for a High Performance General Aviation Airfoil*, NASA CR–2443 (1974).

LES SOLUTIONS DES ÉQUATIONS D'EULER AUX GRILLES NONSTRUCTURÉS POUR L'ECOULEMENT DEUXDIMENSIONEL STATIONAIRE

On a développé la méthode numérique à la résolution des équations d'Euler dans le but de determiner champ d'écoulement stationaire autor des profils aérodynamiques individuels plus composantes. Cette méthode utilise les grilles nonstructures constitués par les élements triangulaires. Les équations d'Euler dans la forme d'integrale se resolvent en utilisant la méthode des volume finis avec inconnus aux centres de gravité des éléments. L'intégration par le temps jusqu à l'état stationaire se fait avec Runge–Kutta de schéma explicite. Pour accéler la convergation on a utilisé les méthodes standards locale des pas de temps, d'assourdissement entalphique et d'average implicite des residus. L'attestation de la méthode a fait pour le test dans le cas subsonique et transonique.

REŠENJA OJLEROVIH JEDNAČINA NA NESTRUKTURISANIM MREŽAMA DVODIMENZIJSKA STACIONARNA STRUJANJA

Razvijena je metoda za numeričko rešavanje Ojlerovih jednačina u cilju određivanja stacionarnog strujnog polja oko pojedinačnih i višekomponentnih aeroprofila. Metoda koristi nestrukturisane mreže sastavljene od trougaonih elemenata. Ojlerove jednačine u integralnoj formi rešavaju se koristeći metodu konačnih zapremina sa nepoznatim u težištima elementa. Integracija po vremenu do dostizanja stacionarnog stanja vrši se eksplicitnom šemom Runge–Kuta. Za

ubrzavanje konvergencije korišćene su standardne metode lokalnog vremenskog koraka, entalpijskog prigušenja i implicitnog osrednjavanja ostatka. Za proveru metode izvršeno je testiranje podzvučnih i transoničnih slučajeva.

Dr Mirko S. Kozić
Cvijićeva 89/16
11000 Belgrade, Yugoslavia